

Broad versus narrow Fano-Feshbach resonances in the BCS-BEC crossover with trapped Fermi atoms

S. Simonucci, P. Pieri, and G.C. Strinati

Dipartimento di Fisica, UdR INFM, Università di Camerino, I-62032 Camerino, Italy

(Dated: February 8, 2020)

With reference to the broad and narrow Fano-Feshbach resonances of ^6Li at about 822G and 543G , we show that for the broad resonance a molecular coupled-channel calculation can be mapped with excellent accuracy onto an effective single-channel problem with a contact interaction. This occurs for a wide enough range of the magnetic field, that the full BCS-BEC crossover can be realized with a typical trap. For the narrow resonance, the mapping onto a single-channel problem *and* the realization of the BCS-BEC crossover are restricted to too narrow a range of the magnetic field to obtain them in practice. In this way, the BCS-BEC crossover for Fermi atoms with the broad resonance is placed on the same footing as the corresponding crossover for different physical systems.

PACS numbers: 03.75.Ss,34.50.Pi,03.75.Hh

Fano-Feshbach (FF) resonances [1] are currently used to control the effective atom-atom interaction in trapped Fermi gases [2, 3, 4, 5], for realizing the BCS-BEC crossover [6, 7, 8] from overlapping Cooper pairs to non-overlapping composite bosons at low enough temperature. Study of this crossover was originally motivated by the condensation of excitons in solids [9], and more recently applied to nuclei [10] and high-temperature superconductors [11].

In this context, a large amount of work has been made by adopting a contact potential for the effective fermion-fermion attraction, regularized in terms of the scattering length a_F [12, 13, 14]. The use of this potential considerably simplifies the many-body diagrammatic structure, both in the normal [13, 14] and broken-symmetry [13, 15] phases. By this approach, only fermionic degrees of freedom are retained in the many-body Hamiltonian, in the same spirit of the original BCS theory [16].

Since just the quantity a_F is varied in a controlled way by sweeping the magnetic field across a FF resonance, it would appear that trapped Fermi gases constitute an ideal testing ground for many-body theories based on the above two-body interaction. Previous theoretical work using the same interaction could thus be adapted to trapped Fermi gases with limited effort.

Use of the *same* effective two-body interaction for such different systems like high-temperature superconductors and trapped Fermi gases may also lead to the emergence of *universal* features. This should be especially desirable, as the insights gleaned from the BCS-BEC crossover with trapped Fermi gases could lead to a better understanding of high-temperature superconductors [17].

Most theoretical work on the BCS-BEC crossover with trapped Fermi gases, however, has been formulated with a fermion-boson model, aiming at incorporating the molecular states coupled in a FF resonance [18]. Inclusion of resonance processes in the BCS-BEC crossover was then named “resonance superfluidity”. This was claimed to result in a different BCS-BEC crossover [19]

from that discussed for high-temperature superconductors. A fermion-boson model was actually proposed some time ago for the study of high-temperature superconductors [20]. This model was, however, conceived to include phenomenologically the coupling of fermions to a boson mode, which represents fluctuations internal to the fermion system (and not a two-fermion state as in resonance superfluidity).

Given the current experimental advances on the BCS-BEC crossover with trapped Fermi atoms, it seems timely and important to settle the issue of which (single- vs multi-channel) model is relevant for an accurate description of this crossover. By performing *ab initio* calculations of molecular ^6Li in the presence of a magnetic field, comparison will be made between the two FF resonances occurring at (about) 822G and 543G , which we shall regard as representative of “broad” and “narrow” resonances, respectively. We will show that, for the broad resonance, the outcomes of the coupled-channel calculation can be mapped with excellent accuracy onto the results of the single-channel model with a contact potential over a wide magnetic field range. On the contrary, for the narrow resonance this mapping can be realized only for too narrow a region of the magnetic field to be experimentally accessible.

These two resonances have been selected to pursue the realization of the BCS-BEC crossover with trapped Fermi atoms (cf. Refs.[2] and [3, 4] for the narrow and broad resonance, in the order). We will conclude that the experimental realization of the BCS-BEC crossover can be made, in practice, only with the broad resonance and that the use of the single-channel model is correspondingly appropriate to describe the crossover. The ultimate reason for the “broad” and “narrow” nature of the FF resonances here considered will also be accounted for.

The key theoretical issue is whether a *minimal* description of many-body effects in these systems can be given in terms of a single-channel model (where the scattering length a_F is the only relevant parameter) or of a multi-

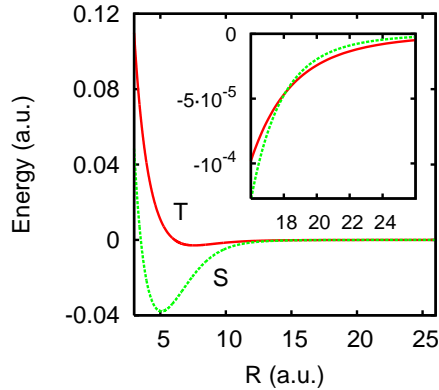


FIG. 1: Molecular energy curves plus (diagonal) hyperfine and Zeeman contributions (taken at 820G) for the singlet (S) and triplet (T) states of lowest energy vs the nuclear separation R . The inset shows the details of the crossing at $R = 18$ a.u..

(possibly two-) channel model (where additional parameters, like the effective range of the potential, appear). In the theory of resonance superfluidity [18], the need for a multi-channel model to describe the BCS-BEC crossover with trapped Fermi atoms was assumed, arguing generically that the energy dependence of two-body scattering matters for this problem [21]. The point is, however, that the experimental conditions introduce the average inter-particle distance as an intrinsic length scale, so that only after combining this length scale with the two-body properties of a given FF resonance one can decide whether the single- or multi-channel model is adequate.

The molecular calculation for the biatomic molecule of ${}^6\text{Li}$ is set up by the Born-Oppenheimer scheme. The auxiliary electronic Schrödinger equation at fixed nuclear separation R is solved via a standard Configuration Interaction method, with zero projection of the total electron angular momentum along the nuclear axis. The coefficient of the R^{-6} tail of the electronic energy curves is fine-tuned (to within a few percent), in order to fix the positions of the FF resonances at the experimental values $(822 \pm 3)\text{G}$ [3, 4] and $(543.23 \pm .05)\text{G}$ [2] (these positions turn, in fact, out to be quite sensitive to the details of the curves for the electronic energy). [In practice, the R^{-6} tail of these energy curves is set to zero for R larger than $R_0 = 4000$ a.u..] With this slight adjustment only, the scattering length is found to have a zero crossing at $B = 533\text{G}$, which is quite close to the experimental value $(528 \pm 4)\text{G}$ [22]. In addition, the calculated hyperfine splitting between the atomic $F = 3/2$ and $F = 1/2$ states turns out to be 217 MHz, to be compared with the experimental value 228 MHz. The nuclear wave equation contains the hyperfine and Zeeman couplings, and is solved only for s -wave relative motion. The low-energy sector relevant to the two FF resonances is thus spanned by five channels, corresponding to the singlet ${}^1\Sigma_g^+$ with

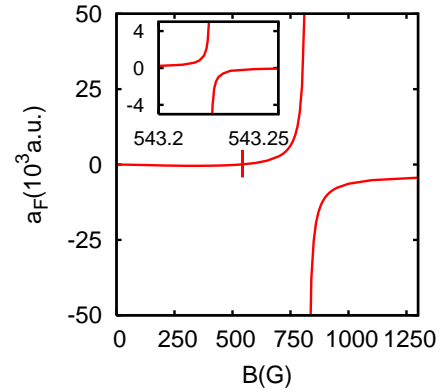


FIG. 2: Scattering length a_F vs magnetic field B . The inset shows the details of the narrow resonance at about 543G.

spin configurations $|0, 0\rangle_e |0, 0\rangle_n$ and $|0, 0\rangle_e |2, 0\rangle_n$ (which will be referred to as the “resonance” channels), and to the triplet ${}^3\Sigma_u^+$ with spin configurations $|1, 1\rangle_e |1, \bar{1}\rangle_n$, $|1, 0\rangle_e |1, 0\rangle_n$, and $|1, \bar{1}\rangle_e |1, 1\rangle_n$ (which will be referred to as the “scattering” channels), for the electronic (e) and nuclear (n) spin functions with $F_z = 0$.

Figures 1 and 2 show representative outcomes of our molecular calculation. In particular, in Fig.1 the (diagonal) hyperfine and Zeeman contributions (taken at 820G) are added to the electronic energy curves of lowest energy for the singlet (S) and triplet (T). Note in the inset the crossing of the two curves induced by the Zeeman coupling, which makes the lowest energy threshold of triplet character. In Fig.2 the calculated scattering length a_F is shown from $B = 0$ to $B = 1300\text{G}$. The inset shows the details of a_F for the narrow resonance at about 543G.

Several quantities of interest can be extracted from this calculation. Below resonance, we compare: (i) The binding energy E_b (obtained from the multi-channel calculation) to the value $\epsilon_0 = (Ma_F^2)^{-1}$ for the contact potential, where M is the nuclear mass; (ii) The corresponding (root-mean-square) radius \bar{R} of the full bound wave function to the value $a_F/\sqrt{2}$ for the contact potential. We also calculate: (iii) The (root-mean-square) radius \bar{R}_2 associated with the component of the total wave function in the resonance channel; (iv) The (squared) projection $|w_1|^2$ of the total wave function in the scattering channel; (v) The corresponding projection $\langle \phi_{\text{cp}} | w_1 \rangle$ onto the bound wave function $\phi_{\text{cp}} = (\sqrt{2/a_F}) \exp(-R/a_F)$ for the contact potential.

Table I reports all these quantities for the two resonances. Note how, for the broad resonance, the effective single-channel model with a contact potential reproduces with excellent accuracy all results obtained by the multi-channel calculation. Note, in particular, how the bound-state wave function of the multi-channel calculation projects almost completely in the scattering channel, which is the sole considered by the effective single-

B (G)	a_F	E_b/ϵ_0	$\sqrt{2}\bar{R}/a_F$	\bar{R}_2/\bar{R}	$ w_1 ^2$	$\langle \phi_{\text{cp}} w_1 \rangle$	r_0
650	1.29	1.068	1.00053	.039	.99669	.972	.085
750	6.26	1.014	1.00004	.008	.99986	.994	.087
800	26.2	1.003	1.00024	.002	.99998	.999	.088
850	-25.3						.088
1100	-5.17						.090
1300	-4.35						.090
.2200	2.09	.0425	1.148	.022	.062	.194	-121
.2210	4.85	.0581	1.517	.007	.134	.289	-121
.2216	41.7	.9066	.5853	.002	.304	.550	-124
.2218	-34.3						-125
.2220	-10.7						-127
.2225	-4.22						-126

TABLE I: Comparison of the molecular calculation with the effective single-channel model, for the broad resonance at about 822G and for the narrow resonance at about 543G. For the narrow resonance, only decimal digits after 543G are reported in the first column. Both a_F and r_0 are in 10^3 a.u..

channel model. The spatial extension \bar{R}_2 of the boson introduced in resonance-superfluidity theory [18] remains instead quite smaller than the extension \bar{R} of the true molecular wave function (which corresponds to the internal wave function of the composite boson). A different situation occurs for the narrow resonance. In this case, the effective single-channel model is appropriate only too close to the resonance for being of practical relevance.

To study the BCS-BEC crossover with FF resonances, the above analysis of the molecular calculation must be complemented by the value of the Fermi wave vector k_F (determined by the total number of Fermi atoms in the trap and the trap frequencies) and by the minimum experimental accuracy for the magnetic field.

Irrespective of the underlying theoretical model, the dimensionless parameter $(k_F a_F)^{-1}$ should exhaust the BCS-BEC crossover within a range ≈ 1 about the unitarity limit at $(k_F a_F)^{-1} = 0$. This is because the BCS (with $a_F < 0$) and BEC (with $a_F > 0$) regimes should be reached when $k_F |a_F| \ll 1$, while in the crossover region $k_F |a_F|$ diverges. To span the crossover, one thus needs to identify (at least) three representative values (say, -1.0, 0.0, and 1.0) of $(k_F a_F)^{-1}$, by tuning the magnetic field that controls the FF resonance. With $k_F = 2 \div 3 \times 10^{-4}$ a.u. for the experiments of Refs. [3] and [4], these values of $(k_F a_F)^{-1}$ correspond approximatively to the magnetic field values (1300, 822, 730)G, which are separated by a step $\delta B \gtrsim 100$ G much larger than the minimum experimental accuracy. For these values of B , the single-channel model is totally appropriate to describe the two-body scattering, as seen from Table I. The situation is reversed for the narrow resonance. In this case, the above values of $(k_F a_F)^{-1}$ are realized by setting the magnetic field at (543.2225, 543.2217, 543.2209)G, with a step

$\delta B \simeq 0.001$ G fifty times smaller than the minimum experimental accuracy [2].

To complete the mapping into the single-channel model, there remains to identify the effective spin states $|\uparrow\rangle_{\text{eff}}$ and $|\downarrow\rangle_{\text{eff}}$. From the molecular calculation, the wave function for the broad resonance is found to be (essentially) a triplet both for electrons and nuclei. This implies the identification $|\uparrow\rangle_{\text{eff}} \leftrightarrow |\frac{1}{2}, -\frac{1}{2}\rangle_e |1, 0\rangle_n$ and $|\downarrow\rangle_{\text{eff}} \leftrightarrow |\frac{1}{2}, -\frac{1}{2}\rangle_e |1, 1\rangle_n$ for the separate atoms, as well as the effective singlet configuration $(|\uparrow\rangle_{\text{eff}}^{(1)} |\downarrow\rangle_{\text{eff}}^{(2)} - |\uparrow\rangle_{\text{eff}}^{(2)} |\downarrow\rangle_{\text{eff}}^{(1)})/\sqrt{2}$ for the pair of atoms (with the labels 1 and 2 referring to the two atoms).

Further information can be extracted from the molecular calculation when the total energy is above threshold. It has been asserted [18] that, in resonance conditions, the scattering length a_F no longer suffices to account for the scattering properties, since these depend strongly on energy. Quite generally, the scattering amplitude takes the form $f(k) = (g(k) - ik)^{-1}$, where the wave vector k is associated with the kinetic energy above threshold. For a contact potential $g(k) = -a_F^{-1}$, while for a multi-channel problem $g(k)$ in the scattering channel contains additional k -dependent terms. In particular, at the lowest order in k , $g(k) = -a_F^{-1} + r_0 k^2/2$ where r_0 identifies the “effective range” of the potential. Near resonance (when $a_F^{-1} \approx 0$), $f(k)$ has a strong k -dependence even in the absence of r_0 . The term $r_0 k^2/2$ begins to matter only when $r_0 k \gtrsim 1$. For the BCS-BEC crossover, a natural cutoff for k is provided by k_F in the weak-to-intermediate coupling regime and by a_F^{-1} in the strong-coupling regime. The term $r_0 k^2/2$ is thus *irrelevant* provided $|r_0| k_F \ll 1$ and $|r_0| \ll |a_F|$. The values of r_0 are reported in Table I for the two resonances. For the broad resonance, r_0 is positive (as it is the case for a potential problem) and remains much smaller than $|a_F|$. For the narrow resonance, none of these properties are verified. Since for the broad resonance the product $r_0 k_F$ is smaller than 10^{-2} (with a typical value $k_F \approx 10^{-4}$ a.u.), we conclude that the energy dependence of the scattering properties (*over and above* that resulting from a contact potential) is actually irrelevant when realizing the BCS-BEC crossover with the broad resonance.

It is, finally, of interest to understand the reason why the resonances here considered are broad and narrow relative to each other. Out of the five channels spanning the low-energy sector, the two $^1\Sigma_g^+$ singlets with spin configurations $|0, 0\rangle_e |0, 0\rangle_n$ and $|0, 0\rangle_e |2, 0\rangle_n$ interact mostly with the $^3\Sigma_u^+$ triplet with spin configuration $|1, \bar{1}\rangle_e |1, 1\rangle_n$. In Fig. 3 the magnetic field dependence of the energy of the last singlet bound state (with 38 nodes) is plotted (dashed line) relative to the threshold of the triplet channel (dotted line) for the case when these channels are completely decoupled. These curves cross each other at (about) 550G. The triplet channel, in addition, is found to have a virtual state at thresh-

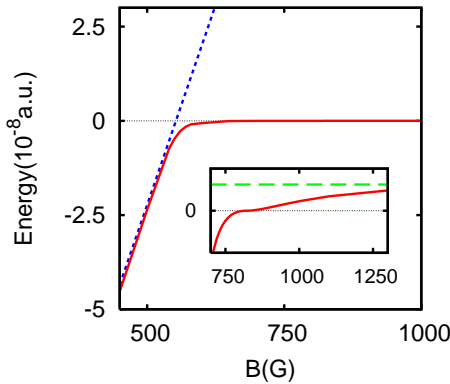


FIG. 3: Mechanism for the occurrence of the narrow and broad FF resonances (see text).

old [23], as the large negative value of the background scattering length a_{bg} indicates ($a_{bg} \simeq -3790$ a.u. when calculated with this channel only). [This value results from our *ab initio* calculation, where the only slightly adjusted parameters are the coefficients of the R^{-6} tail of the electronic energy curves. It differs by about 40% from that reported in the literature [22], where a larger number of adjustable parameters is however used. This difference in a_{bg} does not affect appreciably the values in Table I but for the function $a_F(B)$.]

Out of the two singlet channels, it is always possible to find a linear combination that decouples from the triplet virtual state, thus crossing threshold at (about) 550G. The other combination which couples with the triplet is forced, correspondingly, to have an *avoided crossing* when the interaction between singlets and triplet is restored (full line). The combination which decouples from the triplet results thus in a “narrow” resonance (with a small broadening provided by the coupling to the rest of the continuum states), and maintains its singlet character through the crossing at (about) 550G. The combination which couples with the triplet, on the other hand, acquires (almost) full triplet character past the avoided crossing. For large magnetic field, the energy of the latter tends asymptotically to the broadening $(Ma_{bg}^2)^{-1}$ of the virtual state (long-dashed line in the inset of Fig. 3), thus crossing threshold quite slowly. The slow convergence to the asymptote eventually accounts for the “broad” nature of the resonance vs the magnetic field.

In conclusion, by extracting the relevant information from a coupled-channel calculation for the broad and narrow FF resonances of ${}^6\text{Li}$, a single-channel model with a contact interaction proves adequate to describe the BCS-BEC crossover with the broad resonance. In this way, a connection is established between the BCS-BEC crossover with trapped Fermi atoms and analogous crossovers with other systems. Trapped Fermi atoms are

thus ideally suited for studying the BCS-BEC crossover in a universal fashion, irrespective of mechanisms specific to these simple systems.

This work was partially supported by the Italian MIUR with contract Cofin-2003 “Complex Systems and Many-Body Problems”.

—

- [1] U. Fano, *Nuovo Cimento* **12**, 156 (1935), and *Phys. Rev.* **124**, 1866 (1961); H. Feshbach, *Ann. Phys.* **19**, 287 (1962).
- [2] K.E. Strecker, G.B. Partridge, and R. G. Hulet, *Phys. Rev. Lett.* **91**, 080406 (2003).
- [3] M. Bartenstein, A. Altmeyer, S. Riedl, S. Jochim, C. Chin, J. Hecker Denschlag, and R. Grimm, *Phys. Rev. Lett.* **92**, 120401 (2004).
- [4] M.W. Zwierlein, C.A. Stan, C.H. Schunck, S.M.F. Rupach, A.J. Kerman, and W. Ketterle, *Phys. Rev. Lett.* **92**, 120403 (2004).
- [5] C.A. Regal, M. Greiner, and D.S. Jin, *Phys. Rev. Lett.* **92**, 040403 (2004).
- [6] D.M. Eagles, *Phys. Rev.* **186**, 456 (1969).
- [7] A.J. Leggett, in *Modern Trends in the Theory of Condensed Matter*, A. Pekalski and R. Przystawa eds., Lecture Notes in Physics **115** (Springer, Berlin, 1980), p.13.
- [8] P. Nozières and S. Schmitt-Rink, *J. Low. Temp. Phys.* **59**, 195 (1985).
- [9] C.W. Lai, J. Zoch, A.C. Gossard, and D.S. Chemla, *Science* **303**, 503 (2004), and references quoted therein.
- [10] M. Baldo, U. Lombardo, and P. Schuck, *Phys. Rev. C* **52**, 975 (1995).
- [11] V.M. Loktev, R.M. Quick, and S.G. Sharapov, *Phys. Rep.* **349**, 1 (2001), and references quoted therein.
- [12] C.A.R. Sá de Melo, M. Randeria, and J.R. Engelbrecht, *Phys. Rev. Lett.* **71**, 3202 (1993).
- [13] R. Haussmann, *Z. Phys. B* **91**, 291 (1993).
- [14] P. Pieri and G.C. Strinati, *Phys. Rev. B* **61**, 15370 (2000).
- [15] N. Andrenacci, P. Pieri, and G.C. Strinati, *Phys. Rev. B* **68**, 144507 (2003).
- [16] J.R. Schrieffer, *Theory of Superconductivity* (Benjamin, New York, 1964).
- [17] J.E. Thomas and M.E. Gehm, *American Scientist* **92**, 238 (2004).
- [18] E. Timmermans, K. Furuya, P.W. Milonni, and A.K. Kerman, *Phys. Lett. A* **285**, 228 (2001); M. Holland, S.J.J.M.F. Kokkelmans, M.L. Chiofalo, and R. Walser, *Phys. Rev. Lett.* **87**, 120406 (2001); Y. Ohashi and A. Griffin, *Phys. Rev. Lett.* **89**, 130402 (2002).
- [19] G.M. Falco and H.T.C. Stoof, *Phys. Rev. Lett.* **92**, 130401 (2004).
- [20] J. Ranninger and S. Robaszkiewicz, *Physica B* **135**, 468 (1985).
- [21] S.J.J.M.F. Kokkelmans, J.N. Milstein, M.L. Chiofalo, R. Walser, and M.J. Holland, *Phys. Rev. A* **65**, 053617 (2002).
- [22] K.M. O’Hara *et al.*, *Phys. Rev. A* **66**, 041401(R) (2002).
- [23] The relevance of resonances in the scattering channel was discussed by B. Marcelis, E.G.M. van Kempen, B.J. Verhaar, and S.J.J.M.F. Kokkelmans, cond-mat/0402278.